AGU
ADVANCING EARTH AND SPACE SCIENCE

Earth's Future

Key Points:

- We quantify differences between euphotic-depth-integrated chlorophyll-a (IChl-a) and surface chlorophyll-a (SChl-a) concentrations in the South China Sea
- Inconsistent relationships between IChl-a and SChl-a concentrations between seasons imply caution to use SChl-a for phytoplankton dynamics
- The IChl-a concentration and mixed layer depth could be used as good indices for changes in phytoplankton biomass under climate change

Supporting Information:

Supporting Information may be found in the online version of this article.

Correspondence to:

C.-Y. Ko and F.-K. Shiah,
cyko235@ntu.edu.tw;
fkshiah@rcec.sinica.edu.tw

Effects of Mixed Layer Depth on Phytoplankton Biomass in a Tropical Marginal Ocean: A Multiple Timescale Analysis

Li-Tzu Hou[1], Bo-Shian Wang[2], Chao-Chen Lai[3], Tzong-Yueh Chen[4], Yung-Yen Shih[5], Fuh-Kwo Shiah[3], and Chia-Ying Ko[1,6,7,8] (ID)

[1]Institute of Fisheries Science, National Taiwan University, Taipei City, Taiwan, [2]Marine Science and Information Research Center,, National Academy of Marine Research (NAMR), Ocean Affairs Council, Kaohsiung City, Taiwan, [3]Research Center for Environmental Changes, Academia Sinica, Taipei City, Taiwan, [4]Institute of Marine Environment and Ecology, National Taiwan Ocean University, Keelung City, Taiwan, [5]Department of Applied Science, R.O.C Naval Academy, Kaohsiung City, Taiwan, [6]Department of Life Science, National Taiwan University, Taipei City, Taiwan, [7]Department of Biochemical Science and Technology, Institute of Ecology and Evolutionary Biology, National Taiwan University, Taipei City, Taiwan, [8]Master's Program in Biodiversity, National Taiwan University, Taipei City, Taiwan

Abstract In open oceans, changes in mixed layer depth (MLD) may affect phytoplankton growth and biomass variations via the regulation of nutrient supply from deep waters. Estimates of relationships between variability in phytoplankton dynamics and the MLD remain limited, especially at different time scales. We compiled and analyzed averaged euphotic-depth-integrated chlorophyll-a (IChl-a) and surface chlorophyll-a (SChl-a) concentrations collected from 27 cruises during the period of 1999–2019 in the tropical northern South China Sea (SCS). Seasonal differences existed in both averaged IChl-a and SChl-a concentrations, with significantly high concentrations in the cold season. Inconsistent relationships between the averaged IChl-a and SChl-a concentrations between seasons implied that the use of SChl-a concentration as a common indicator of phytoplankton biomass dynamics should be performed with caution. Over the past decades in the northern SCS, the averaged IChl-a, SChl-a, and MLD decreased to a greater extent in the cold season than in the warm season, while sea surface temperature (SST) rose rapidly and dramatically in both seasons. The MLD was observed to have better correlations with the averaged IChl-a and SChl-a concentrations than the SST in the time-series data. Our results highlight the importance of IChl-a concentration, which is an overall measure of phytoplankton responses to euphotic zone conditions, and the MLD could be used as a good index for changes in phytoplankton biomass under climate change.

Plain Language Summary Given that ocean stratification, corresponding to mixed layer depth (MLD), is critical of phytoplankton growth and biomass variations under climate change, particularly in tropical and subtropical regions, it is important to examine MLD influences on phytoplankton at multiple temporal scales in those areas. Based on long-term investigation in the northern South China Sea during the 1999–2019 period, the identification of oceanographic links with phytoplankton, especially its biomass represented by chlorophyll-a (Chl-a) concentrations, revealed that high Chl-a concentrations in the cold season and typhoon disturbance could play an important role in increasing oceanic production. The interannual and decadal observations showed a progressive increase in sea surface temperature and decreases in both MLD and Chl-a concentrations that may become a severe environmental and biotic crisis in the SCS. To better address contemporary climatic threats, measurements of phytoplankton responses in the euphotic zone remain essential and may not be simply replaced by recent satellite remote sensing development.

1. Introduction

Changes in thermal stratification patterns, such as length of growing season and vertical mixing processes corresponding to mixed layer depth (MLD), have become major factors affecting phytoplankton growth and biomass variations under climate change, particularly in tropical and subtropical oceans (Calbet et al., 2015; Hadfield & Sharples, 1996). Studies have shown that an increase in stratification limits nutrient supply, leads to decreases in phytoplankton biomass and productivity, and further alters food chains and values of marine ecosystem services (Boyce et al., 2010; Schofield et al., 2018; Winder & Sommer, 2012). Phytoplankton are the ultimate source of organic materials driving food-web processes and ecosystem properties, and they account for approximately half of global primary production, amounting to approximately 50 Pg of carbon per year (Field et al., 1998). The

Methodology: Li-Tzu Hou, Bo-Shian Wang, Yung-Yen Shih, Fuh-Kwo Shiah, Chia-Ying Ko
Writing – original draft: Li-Tzu Hou, Bo-Shian Wang, Chao-Chen Lai, Fuh-Kwo Shiah, Chia-Ying Ko

biomass and distribution of phytoplankton can successively impact higher trophic levels, fisheries, and whole ecosystems (Boyce et al., 2010). However, the phytoplankton trends reported by either satellite or field observations at various locations still exhibit high variability at long-term seasonal, interannual and/or decadal time scales (Boyce et al., 2010; Chavez et al., 2011; Schollaert Uz et al., 2017), showing that temporal and spatial heterogeneity may influence the assessment of thermal stratification dynamics and phytoplankton changes.

Since the 1970s, satellite ocean color sensors have provided large-scale and long-term observations and are currently widely applied to detect phytoplankton biomass and distribution (McClain, 2009; Siegel et al., 2013). It is commonly inferred from measurements of total chlorophyll-a (Chl-a) pigment concentration, thus representing variances in marine primary production and capturing the first-order changes in phytoplankton in marine ecosystems (Boyce et al., 2010; Falkowski & Raven, 2013). However, this method has limitations both in relation to the upper water layers and in relation to dynamic detection at an hourly time scale. Therefore, in situ field sampling is expected to more accurately capture phytoplankton dynamics throughout the whole water column, although this type of sampling is difficult and costly to conduct. In general, surface chlorophyll-a (SChl-a) concentrations based on satellite observations are widely used to infer phytoplankton biomass dynamics in most large-scale long-term studies, while euphotic-depth-integrated Chl-a (IChl-a) concentrations, which are instead based on in situ field sampling, can reflect entire vertical distributions of phytoplankton biomass dynamics in the euphotic zone (Frolov et al., 2012; Morel & Berthon, 1989; Uitz et al., 2006).

Recently, studies have highlighted not only importance of the MLD for determining temperature ranges in oceanic and coastal regions and as a source of heat that drives global variability, but also the MLD in relation to vertical stratification for available light and nutrient for marine organisms (Gardner et al., 1995; Jeronimo & Gomez-Valdes, 2010; Sirevaag et al., 2011). Moreover, warming temperatures could cause increases in stratification and a shallowing of the MLD, hence less light and nutrient available for phytoplankton in the mixed layer, which then lead to a decrease of phytoplankton growth (Boyce et al., 2010; Winder & Sommer, 2012). However, too many factors come into play in the oceans, inconsistencies between the MLD and sea surface temperature (SST) in terms of patterns and increasing/decreasing rates have been gradually observed (Somavilla et al., 2017), raising debates regarding how best to consider parameters as representative of contemporary ocean warming and to link with phytoplankton dynamics in oceans. As commonly assumed for simplicity, the mixed layer deepens due to the effects of wind and heat loss to atmosphere but does not shoal smoothly (Price et al., 1986). Instead, the upper ocean stratifies due to solar heating or other heat sources (e.g., freshwater flux), and eventually, a new mixed layer reforms from the surface, thereby isolating phytoplankton and other particles in the so-called remnant layer (C. Ho & Marra, 1994; Lacour et al., 2019). That is, simply, the variability in MLD in fact involves a subtle interplay between circulation and atmospheric forcing (Schofield et al., 2018). In addition, in a comparison at different time scales, the amplitude of MLD variation at a diurnal time scale is usually small (Woods & Onken, 1982), whereas at seasonal and annual scales, the MLD effect becomes a process of greater significance (Carlson et al., 1994; Dall'Olmo & Mork, 2014; Dall'Olmo et al., 2016). Few studies, however, have placed the MLD influence in a time scale-dependent context or have assessed relationships between the MLD and phytoplankton at multiple temporal scales within a marine ecosystem.

The South China Sea (SCS), one of the largest marginal seas in the world, has high marine primary and fisheries production, but strong seasonal monsoons and adjacent oceanic currents make it sensitive to climate variability (K.-K. Liu et al., 2002; Qiu et al., 2010; Tseng et al., 2005). Together with year-round SCS Warm Current and Kuroshio intrusion, the northeast monsoon in winter drives a cyclonic gyre in the SCS, while the southwest monsoon in summer causes a reversal of the gyre in the southern part of the basin (Figure 1; Shaw & Chao, 1994), thereby supporting the role of seasonal, even longer temporal, changes in the area variations in evaporation and precipitation, leading to significant thermal stratification dynamics (Wong et al., 2015). The South East Asia Time-series Study (SEATS) station located at 116°E and 18°N was established to monitor long-term biogeochemical changes in the northern SCS, and regular field observations have been collected since 1999. Previous studies have noted that the depth of thermocline may be a major factor in phytoplankton variability at the SEATS station at a monthly time scale; additionally, the reported MLD at the SEATS station was approximately 20 m deep in summer and 70 m deep in winter, which is relatively shallow compared to the global averaged MLD (Tai et al., 2017; Wong et al., 2015; Wu et al., 2003). Moreover, satellite observations showed Chl-a peaks in both winter and summer, especially in monsoon season (Pan et al., 2015; Wong et al., 2015), resulting in a seasonal pattern distinct from those of other oceans at tropical latitudes (Tseng et al., 2005). Stratification induced by a
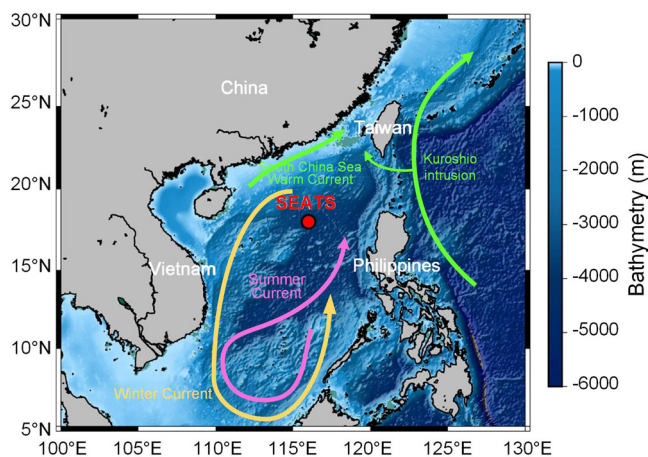
Figure 1. Bathymetric map of the South China Sea and location of the South East Asian Time-series Study (SEATS) station. The map was generated using GMT (Generic Mapping Tools). Both the Kuroshio intrusion and the South China Sea Warm Current are year-round flows (green lines) with different strengths in different seasons. Specifically, there is a branch of the Kuroshio (white line) flowing persistently along the west coast of Taiwan during wintertime. A cyclonic (counterclockwise) gyre dominates the full South China Sea (SCS) basin in the winter (yellow line), while summertime circulation mainly consists of a cyclonic gyre (pink line) in the northern SCS.

combination of temperature and wind also regulated negative correlations between monthly and annual averaged SST and MLD (Tai et al., 2017). Given that the euphotic zone at the SEATS station can be as deep as 100 m in the ocean and that the Chl-a maximum layer is approximately 60 m, which is not close to the surface (K.-K. Liu et al., 2013), the IChl-a concentrations might more accurately represent the dynamics of phytoplankton distribution and biomass in the water column than the surface values in the SCS.

The objectives of this study were (a) to compare differences between IChl-a and SChl-a concentrations and (b) to explore effects of the MLD on both IChl-a and SChl-a concentrations and its potential use as an indicator in comparison to the commonly used SST parameter, particularly at extended time scales, for example, seasonal and decadal scales. We compiled data from 27 cruises at the SEAT station in the northern SCS over two decades, from 1999 to 2019, to identify in situ patterns linking phytoplankton and ocean-ographic variables, including SST and MLD. In addition, due to long-term impacts of climate change, which is becoming a greater threat in the Anthro-pocene (IPCC, 2013; Pörtner et al., 2014), we further hypothesized that at these extended time scales, high correlations should exist between phyto-plankton and MLD because of ocean mixing as a better parameterization for modeled oceanic stratification and resultant biological carbon storage (Oka & Niwa, 2013; Tatebe et al., 2018).

2. Materials and Methods

2.1. Field Sampling

Phytoplankton and oceanographic measurements collected at the SEATS station in the northern SCS were compiled from 27 cruises over the course of more than two decades (1999–2019; Table S1 in Supporting Information S1). Sea temperature and Chl-a fluores-cence data were continuously recorded by a conductivity-temperature-depth (CTD) profiling recorder (Sea-Bird model SBE9/11, Sea-Bird Electronics, Inc.), corresponding to one measurement per meter of water depth, during every cast in each cruise. Laboratory calibrations of all CTD sensors were done before each cruise and two sets of the CTD recorders were set up onboard in each cruise for simultaneously monitoring and comparing real-time estimates. The surveyed casts conducted during each cruise with sampling frequencies ranged from 3 to 6 hr over a 13-hr to 4-day period.

2.2. Phytoplankton Chl-a Biomass Measurement

Water samples for in situ phytoplankton Chl-a biomass measurements were taken from depths of 5, 10, 20, 30, 50, 80, and 100 m. The samples were filtered onboard through 47-mm GF/F filters (Whatman) under a vacuum pressure of less than 100 mmHg and preserved at $-20°C$ until further processing. In the laboratory, the filters were extracted by 90% acetone and measured either by high-performance liquid chromatography (HPLC; Shimazu LC-10A, method refers to T.-Y. Ho et al., 2015) or by a fluorometer (Turner 10-AU, method refers to Strickland & Parsons, 1972), with the Chl-a standard validated by a UV-vis spectrophotometer and fluorometer for calibration. Both HPLC and fluorometer methods are well developed for measuring marine Chl-a concentra-tions, and their measured results are comparable (Murray et al., 1986). To derive phytoplankton Chl-a biomass within the euphotic zone, readings from an onboard CTD fluorescence meter were calibrated with discrete in situ Chl-a measurements using least squares linear regression. The coefficients of determination in the 27 cruises ranged from 0.42 to 0.97 (Figure S1 in Supporting Information S1). The calibrated Chl-a fluorescence values were finally used to represent phytoplankton biomass dynamics in the following analyses. To limit perturbations caused by wave height, the Chl-a concentrations at a depth of 10 m were then used as surface measurements in this study. The averaged IChl-a concentrations as the euphotic-depth measurements were calculated by a trape-zoidal integration method taking average from depths of 10–100 m (Uitz et al., 2006).
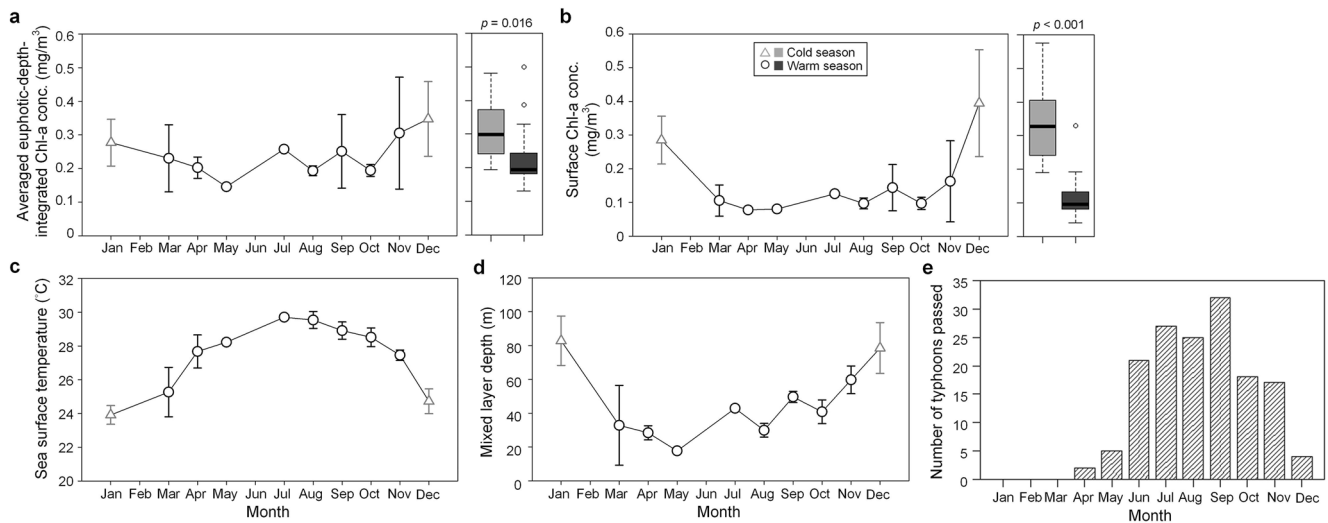
Figure 2. Monthly and seasonal variations in the average (±1 standard deviation, SD) (a) averaged euphotic-depth-integrated chlorophyll-a (Chl-a) concentration, (b) surface Chl-a concentration, (c) sea surface temperature, (d) mixed layer depth, and (e) number of typhoons passing through waters surrounding the South East Asia Time-series Study station (±5° latitude and longitude) in the northern South China Sea. There were no cruises conducted in February and June during the study period of 1999–2019. Dark and light gray colors indicate cold (December-January) and warm (March-November) seasons, respectively. Boxplots represent the median (bar), interquartile range (box), non-outlier range (whiskers), and outliers (circles) for Chl-a concentrations. Differences (*p*-values) in Chl-concentrations between seasons are shown according to the Wilcoxon signed-rank test. The typhoon records were compiled from the National Institute of Informatics (agora.ex.nii.ac.jp) from 2009 to 2018.

2.3. Data Management and Statistical Analysis

All surveyed casts were first systematically analyzed for characterizing diurnal-scale changes. To eliminate biased diurnal sampling effort due to sea conditions, only daytime casts implemented between 08:00 and 16:00 and nighttime casts between 20:00 and 04:00 were selected to standardize variability. The MLD was defined as depth at which the sea temperature cooled by 0.8°C relative to that at 10 m depth, that is, $\Delta T = 0.8°C$ (Tai et al., 2017).

To validate in situ measurements to a larger spatial scale, satellite Chl-a data were compared using daily MODIS-Aqua 4-km level 3 observations and assimilated monthly Chl-a data from the three-dimensional NASA Ocean Biogeochemical Model (NOBM) coupled circulation/biogeochemical/radiative processes of global oceans (Gregg, 2008). Both satellite Chl-a concentrations were mapped within a spatial range of 115.5°−116.5°E, 17.5°−18.5°N and a temporal range of July 2002 to December 2019.

Differences in SChl-a and averaged IChl-a concentrations between seasons were quantified using the Wilcoxon signed-rank test. Relationships among SChl-a, averaged IChl-a, and satellite Chl-a concentrations and changes in both SChl-a and averaged IChl-a concentrations and oceanographic variables, that is, MLD and SST, over time were estimated using regressions. Pearson's correlations between seasonal and interannual Chl-a concentrations and oceanographic variables were also assessed. The *p*-value lower than 0.05 was considered to be statistically significant. All statistical analyses were carried out by R 3.6.2 (R Core Team, 2019).

3. Results and Discussion

3.1. Intra-Annual Dynamics

At the SEATS station, the monthly averaged IChl-a concentrations ranged from 0.146 mg m^{-3} in May to 0.347 mg m^{-3} in December, and the monthly SChl-a concentrations ranged from 0.078 mg m^{-3} in December to 0.395 mg m^{-3} in April (Figures 2a and 2b), while the monthly averaged SST had a bell-shaped distribution with a peak of 29.71°C in July and a record low of 23.91°C in January (Figure 2c) and an opposite trend for the MLD (17.67 and 81.83 m in May and January, respectively; Figure 2d). The observed Chl-a pattern was similar to middle- and high-latitude open ocean water dynamics, such as the Bermuda Atlantic Time-series Study and the Hawaii Ocean Time-series station ALOHA, where phytoplankton biomass increase when the deep MLD penetrates the nutricline, which allows nutrients to enter the upper mixed layer in winter, and a shallower MLD causes low

Chl-a concentrations in nutrient-limited surface waters in summer (Chavez et al., 2011; Cullen, 2015; Karl & Church, 2014). The intra-annual Chl-a dynamics in the SCS are caused by the consistent year-round solar irradiance, winter convective overturn by surface cooling, the influences of monsoon-enhanced wind-induced mixing with the strongest upwelling in winter and weak upwelling in summer, and cyclonic eddies caused by the Kuroshio intrusions during winter, which trigger phytoplankton blooms (Chen et al., 2006; M. Liu et al., 2015; Pan et al., 2015; Tseng et al., 2005).

Two seasons, that is, cold and warm, were classified at the SEATS station based on vertical oceanographic profiles (Figures S2 and S3 in Supporting Information S1). In the cold season (December and January), SSTs were lower than 27.5°C, water column was generally well mixed, and Chl-a fluorescence showed a uniform vertical profile with a relatively even distribution of high concentrations above the MLD in the upper 50 m of the water column. In the warm season (March to November), SSTs were higher than 27.5°C, waters showed stratification above a depth of 60 m, and the peak Chl-a fluorescence or subsurface Chl-a maximum layer existed at subsurface depths of 50–80 m, which were below the MLDs.

Significantly higher median values of the averaged IChl-a and SChl-a concentrations were observed in the cold season than in the warm season (both $p < 0.05$, Figures 2a and 2b). Larger differences between the two seasons existed in SChl-a concentrations (with a difference of approximately 3.1 times) than in averaged IChl-a concentrations (with a difference of approximately 1.4 times), indicating consistent active phytoplankton growth and activity in the upper euphotic water layers year round in the northern SCS. These variations between SChl-a and IChl-a concentrations could be due to differences in the strengths of monsoons, which are strong in the cold season and weak in the warm season, inducing mixing and winter convective overturning by surface cooling, leading to low SChl-a values and high Chl-a peaks at the subsurface nutricline (Pan et al., 2015; Tseng et al., 2005).

The small differences in averaged IChl-a concentrations between seasons at the SEATS station and the similarity between values observed in the warm season, particularly in July, September, and November, and those in the cold season may be due to episodic events, including typhoons and mesoscale processes, that alter phytoplankton community responses and succession (Alford et al., 2015; Zhao et al., 2008). We found typhoon disturbances with monthly cumulative numbers ranging from 2 to 32 in recent decades in the SCS (Figure 2e). Lin et al. (2003) proved that after a modulated typhoon passed, oceanic processes, including water mixing, uplift of nutrients from below the thermocline, and phytoplankton growth and activity in the water layers, caused phytoplankton biomass in the warm season to be comparable to that in the cold season, although Chl-a blooms were usually short lived and small in extent and not induced if nutrients at the sea surface were limited. The post-typhoon periods play an important role in the timeline of phytoplankton increases, and seasonal variation has also been observed in different aquatic ecosystems (C.-Y. Ko et al., 2017). Moreover, unlike previous studies showing the importance of mesoscale processes such as thermal fronts and eddies in the waters surrounding the northern SCS (Owen, 1981; Xian et al., 2012; Ye et al., 2017), we found that these processes rarely caused detectable Chl-a concentration anomalies among the 27 cruises in this study (Table S1 in Supporting Information S1). Only the OR1-664 cruise in November 2002 showed impacts of ENSO events on diurnal phytoplankton fluctuations with dramatically high hourly averaged IChl-a and SChl-a concentrations (Figure S4 in Supporting Information S1); these findings may challenge understandings of anti-cyclonic ocean circulation existing in the SCS outside the aforementioned monsoon seasons, similar to the rare and special physical oceanographic conditions such as a combination of cold SST pool and peak in upwelling that occurred in the SCS in spring 2003 and autumn 2010 (D. S. Ko et al., 2014; Lin et al., 2003). Future work is needed to disentangle multiple ecological mechanisms and environmental stressors at play, including estimations of time-lag effects, different atmospheric scales, and potential feedbacks, to provide insights into the process of phytoplankton biomass dynamics during the observed patterns.

Interestingly, when estimating the relationships between averaged IChl-a and SChl-a concentrations, seasonal differences were observed, with a higher R^2 value in the warm season than in the cold season (Figure 3a). Therefore, the SChl-a concentrations might not fully reveal vertical distributions of phytoplankton biomass, at least at the seasonal scale, and should be used with caution as an indicator of phytoplankton biomass dynamics. Moreover, the widely used satellite Chl-a concentrations, either assimilated monthly, that is, NOBM Chl-a, or daily, that is, MODIS Chl-a, showed limited predictive power, except for the SChl-a versus NOBM Chl-a concentrations in the warm season ($R^2 = 0.44$), and revealed considerable variability in the Chl-a concentrations in the surface waters (Figures 3b and 3c). These results suggest that in the northern SCS, phytoplankton biomass and/or primary production derived from satellite Chl-a data could be underestimated, because the satellite
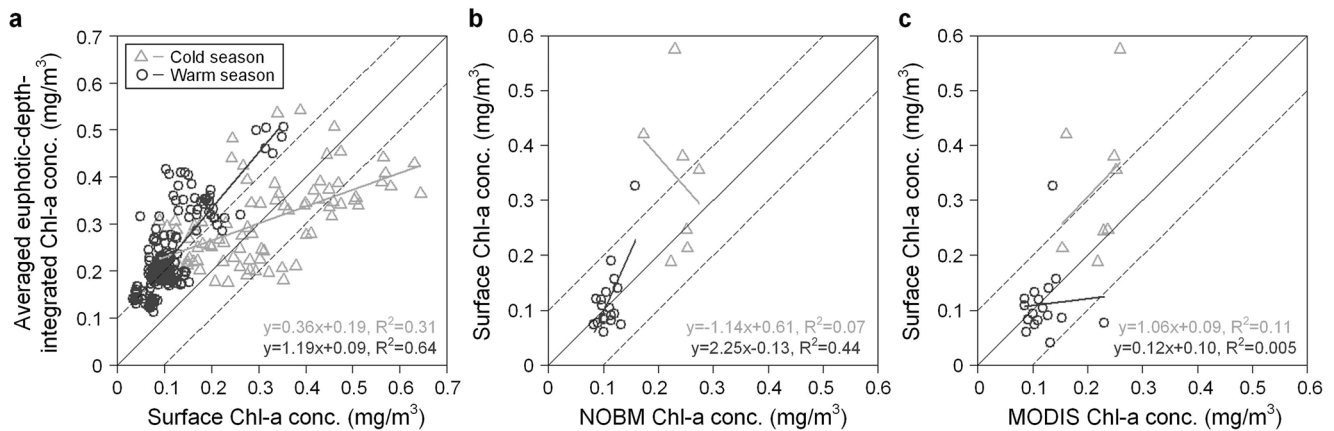
Figure 3. Relationships among in situ averaged euphotic-depth-integrated, surface and satellite assimilated monthly, that is, NOBM, and daily, that is, MODIS, chlorophyll-a (Chl-a) concentrations at the South East Asia Time-series Study station in the northern South China Sea in cold (triangle) and warm (circle) seasons during the study period from 1999 to 2019. Thick solid lines indicate seasonal regressions, and thin gray solid and dashed lines indicate 1:1 agreement and ± 0.1 ranges, respectively. The seasonal regression models and estimated R^2 values are shown.

measurements are optical depth-averaged values of the upper water column and usually without consideration for vertical variations (Gordon et al., 1980; Lee & Carder, 2004; Ma et al., 2014). We suggest that such derivation formulas using remote sensing and satellite technology provide an easily accessible but highly heterogeneous uncertainty that will require careful calibration of samples. Scientists have been trying to uncover the vertical distributions of phytoplankton and depth-integrated primary production (IPP) by surface Chl-a data (Behrenfeld & Falkowski, 1997; Morel & Berthon, 1989; Saba et al., 2010; Uitz et al., 2006). Recently, a surprisingly strong relationship between SChl-a and averaged IChl-a concentrations was observed to hold for profiles with high concentrations of Chl-a in persistent thin (<3 m) subsurface phytoplankton layers in California (Frolov et al., 2012). Besides, complexity of physical-oceanographic processes, variability of phytoplankton physiology, and biological interactions in the phytoplankton community can cause highly heterogeneous shifts in the water layers (Cullen, 2015; Frolov et al., 2012; Gittings et al., 2018; Vanharanta et al., 2020). Therefore, unraveling the relationships between changes in phytoplankton biomass in the surface and euphotic-depth water layers in the northern SCS still needs to be conservative and open to adjustment to account for other factors.

3.2. Interannual Trends and Decadal Variations

From 1999 to 2019, both averaged IChl-a and SChl-a concentrations decreased to a greater extent in the cold season than in the warm season, with the averaged IChl-a concentrations decreasing more than the SChl-a concentrations (Figure 4; decreases per decade: -0.084, -0.058, -0.071, and -0.053 mg m^{-3}; slopes of regression lines: -0.009 ($F_{(1, 59)} = 21.73$; $p < 0.001$), -0.006 ($F_{(1, 160)} = 28.25$; $p < 0.001$), -0.0077 ($F_{(1, 59)} = 4.03$; $p = 0.049$), and -0.0054 ($F_{(1, 160)} = 58.11$; $p < 0.001$), representing averaged IChl-a concentrations in the cold and warm seasons and SChl-a concentrations in the cold and warm seasons, respectively). The SST in the northern SCS had risen rapidly and dramatically in recent decades, with increases per decade at 0.95°C and 0.77°C and slopes of regression lines at 0.09 ($F_{(1, 59)} = 36.19$; $p < 0.001$) and 0.071 ($F_{(1, 160)} = 10.57$; $p = 0.001$) in the cold and warm seasons, respectively, both exceeding the global average of 0.11°C per decade from 1971 to 2010 in the Fifth Assessment Report (AR5) of the Intergovernmental Panel on Climate Change (IPCC, 2013). The MLD showed the greatest decreases, with decreases per decade at -13.91 and -4.07 m and regression lines with slopes of -1.422 ($F_{(1, 59)} = 27.15$; $p < 0.001$) and -0.4703 ($F_{(1, 160)} = 4.64$; $p = 0.033$) in the cold and warm seasons, respectively, indicating large in situ decreases in the temperature range in the northern SCS oceanic regions and impacts of heat storage within the northern SCS mixed layer over time.

Our results support the conclusions from Boyce et al. (2010) and Tai et al. (2017), who reported that with observed and projected increases in SST (Boyce et al., 2010; Pörtner et al., 2014), the warming of the surface ocean waters with stratification in tropical and subtropical oceans could reduce vertical mixing of the upper water layer, causing a shallower MLD and reducing nutrient input into the surface waters, thereby resulting in a decrease in phytoplankton biomass and productivity in both the surface and euphotic-depth layers. However,
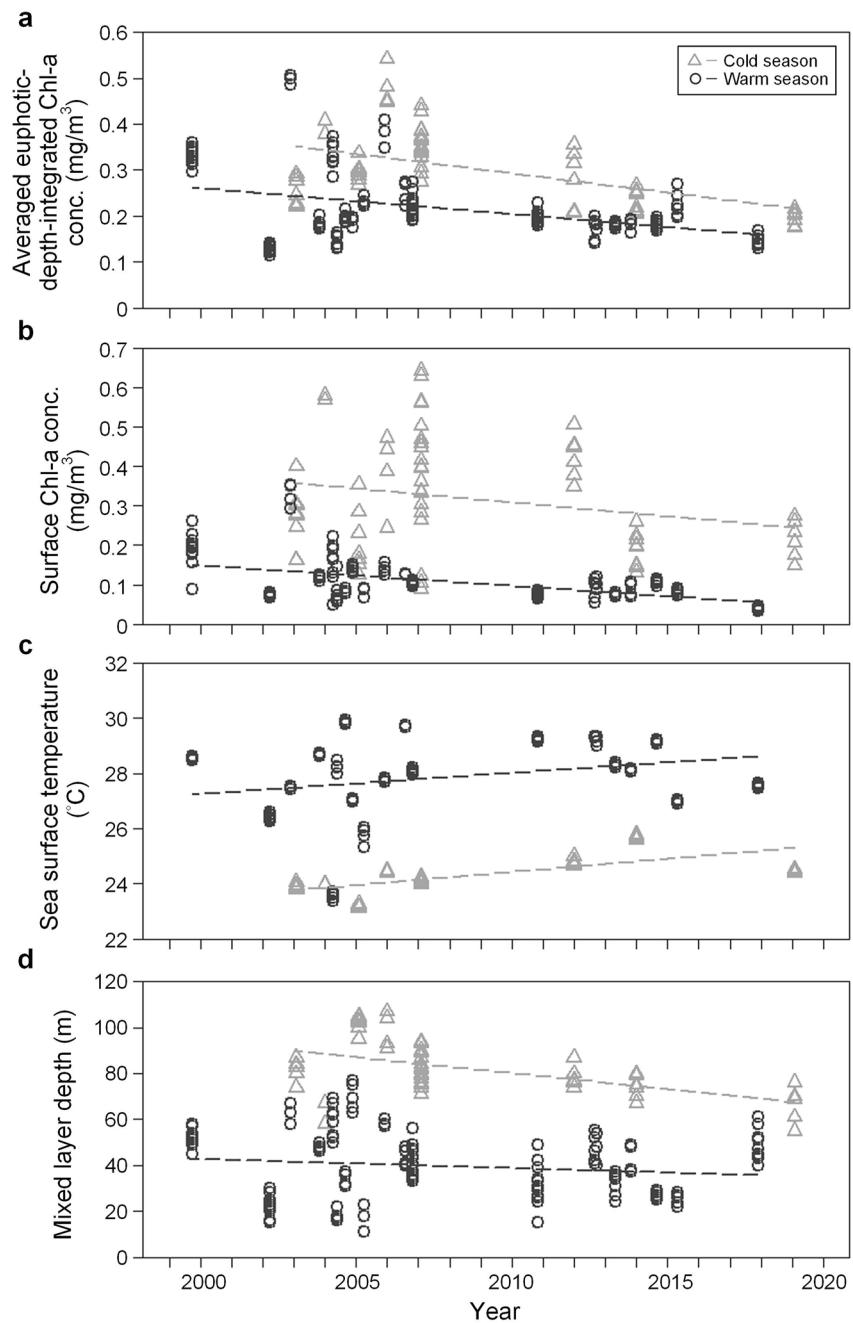
Figure 4. Decadal trends in in situ (a) averaged euphotic-depth-integrated chlorophyll-a (Chl-a) concentration, (b) surface Chl-a concentration, (c) sea surface temperature, and (d) mixed layer depth at the South East Asia Time-series Study station in the northern South China Sea during the study period of 1999–2019. Individual triangles and circles indicate every cast during each cruise. Trends in cold and warm seasonal series are shown by light and dark gray dashed lines, respectively.

the North Pacific subtropical gyres, the North Atlantic, and the mid-latitude Eastern North Atlantic did not show significant changes in the MLD and IChl-a concentrations with respect to the increased SST in recent decades, where changes in salinity, density, wind-driven divergence and buoyancy losses could have more dominant effects (Chavez et al., 2011; Somavilla et al., 2017). Increasing SST can cause plankton community compositions to shift toward small-sized phytoplankton and cyanobacteria (Rasconi et al., 2015) and alter phytoplankton stoichiometry and metabolism (Toseland et al., 2013; Winder & Sommer, 2012), both of which also contribute to a decrease in phytoplankton biomass. In addition, despite increasing fishing effort after the 1990s, the fisheries in the SCS
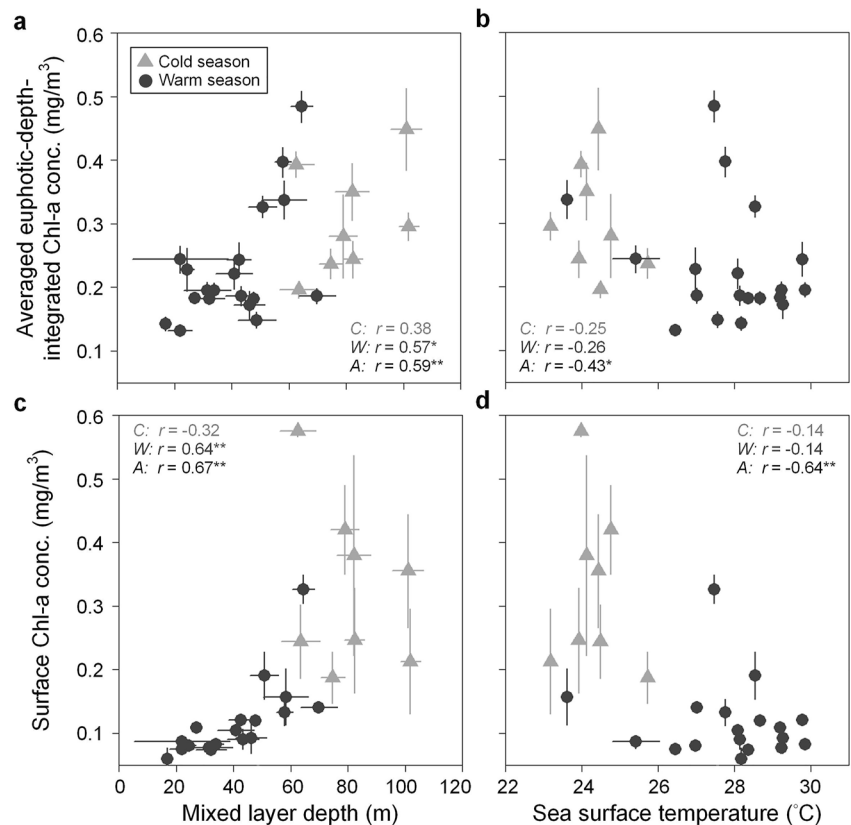
Figure 5. Relationships among averaged euphotic-depth-integrated and surface chlorophyll-a (Chl-a) concentrations, mixed layer depth, and sea surface temperature. Triangles and circles indicate means in cold and warm seasons, respectively, and error bars indicate ±1 standard deviation (SD) for each cruise at the South East Asia Time-series Study station in the northern South China Sea during 1999–2019. Numbers in the figures correspond to Pearson's correlation coefficients and significance (*$p < 0.05$; **$p < 0.01$) in annual (A), cold (C), and warm (W) seasonal series.

stagnated, and the mean temperature of catch did not increase with SST, in contrast to the pattern observed in other subtropical large marine ecosystems (Pauly & Liang, 2020). As a consequence, the severe effects of such SST increases, accompanying decreases in phytoplankton biomass, contribute to associated food chain disturbance and a more vulnerable SCS marine ecosystem under climate change. Accordingly, as a semi-enclosed marginal sea with little water exchange potential and consistently great fishing pressure, the SCS may be especially prone to contemporary increases in SST and decreases in MLD. We caveat that the continuous decreases in phytoplankton biomass may become a severe biotic crisis in the SCS.

Investigation of changes in the interannual variabilities in Chl-a concentrations in response to SST and MLD forcing revealed that both averaged IChl-a and SChl-a concentrations were inversely correlated with SST but positively correlated with MLD, with varied correlations ranging in magnitude from −0.26 to 0.64, −0.14 to 0.38, and −0.64 to 0.67 in the warm season, cold season and all years, respectively (Figure 5). These strong correlations between Chl-a and SST and MLD also prevailed at low latitudes, as observed in previous studies (Boyce et al., 2010; M. Liu et al., 2015; Schollaert Uz et al., 2017). Our findings demonstrate that the MLD is a more significant and stronger predictor of Chl-a concentrations than SST in time-series data, although this relationship exhibits regional variability in response to modern disturbance trends (Hadfield & Sharples, 1996; Jeronimo & Gomez-Valdes, 2010; Tai et al., 2017). Notably, with different magnitudes of correlation coefficients in SST and MLD, the higher annual correlations observed between the averaged IChl-a concentrations and SST and MLD than those observed based on SChl-a concentrations. However, differently, high seasonal correlations existed between the SChl-a concentrations and SST and MLD, again indicating that the use of SChl-a concentrations to represent ocean water conditions derived from satellite remote sensing may require more consideration. Considering that physical oceanographical processes such as SST and MLD are usually easier to monitor and predict

changes than biological processes and that the MLD directly represents nutrient availability in the euphotic zone, especially in oligotrophic open oceans (Tai et al., 2017; Wu et al., 2003), our analysis thus emphasizes the use of MLD to represent water column phytoplankton biomass and/or primary production under climate change. Furthermore, the averaged IChl-a concentrations were more tightly coupled with MLD than with SST, robustly demonstrating that the use of MLD could better predict oceanic Chl-a vertical concentrations, although the afore-mentioned seasonal dynamics between these oceanographic variations and phytoplankton performance exist. Overall, these findings add an important time scale context to previous work on MLD or SST correlations with observed phytoplankton changes and highlight the complexity of interactions between time scales and consequences of phytoplankton biomass changes.

Apart from long-term temporal changes, another interesting observation in this study was large diurnal variations among cruises and between seasons at the SEATS station in the northern SCS (Figure S4 in Supporting Information S1). Specifically, in the cold season, high Chl-a concentrations were shown in the late evening, and low concentrations occurred before noon. Similar trends were reported in the equatorial Pacific (Claustre et al., 1999; Neveux, 2003; Vaulot & Marie, 1999), the North Pacific Ocean (Siegel et al., 1989), and the North Atlantic (Gardner et al., 1995) by the combined influences of changes in phytoplankton biomass on growth production and losses due to grazing, sinking, and aggregation and phytoplankton photoacclimation and photoinhibition processes in response to diurnal light availability (Claustre et al., 1999; Letelier et al., 1993; Mignot et al., 2014; Neveux, 2003). On the other hand, the warm season cruises did not show a clear diurnal Chl-a pattern with respect to sunlight or time. The diurnal fluctuations in the cold season were more than two-fold higher than those in the warm season, where the diurnal variation could range from 0.09 to 0.64 mg m^{-3} in the SChl-a concentrations within a 17-hr period (Cruise OR1-821, January 2007). Notably, at the SEATS station, the individual samplings around dawn might underestimate the diurnal SChl-a and averaged IChl-a concentrations, while those in the evening might overestimate these Chl-a concentrations, especially in the cold season. Therefore, we suggest that when investigating the short-term variability in phytoplankton dynamics, it is important to not only consider the diurnal effects but also be aware that a single in situ sampling event in the field may not be suitable to adequately represent the diurnal averaged concentrations. Simultaneously, weak interactions between averaged IChl-a and SChl-a concentrations and SST (all $r < -0.2$; Figure S5 in Supporting Information S1) and inconsistent interactions between averaged IChl-a and SChl-a concentrations (r ranging from 0.01 to 0.55; Figure S5 in Supporting Information S1) and MLD were found at hourly and diurnal timescales, further indicating that using SST and MLD to reflect phytoplankton biomass may be inadequate at short temporal scales.

Besides, variability of phytoplankton biomass in the face of primary production has been posed a number of relevant questions and different correlations between them usually exist in different seasons, climatic events, and regions (C. Ho & Marra, 1994; C.-Y. Ko et al., 2017; K.-K. Liu et al., 2002; Lin et al., 2003; Marañón et al., 2003). Austria et al. (2018) found a significant relationship between IChl-a concentrations and euphotic-depth-IPP based on one summer (Jun 2010) and two winter (January and December 2011) cruises conducted at the shelf of the SCS and further indicated that approximately 34% of IPP variations could be explained by the IChl-a concentrations at the SEATS station. We, therefore, believe that the phytoplankton biomass proxy, that is, the IChl-concentrations, presented in this study could be the indexes for rate parameters such as phytoplankton growth and primary production in the northern SCS.

4. Conclusions

The identification of oceanographic links with phytoplankton, especially its biomass, accounting for differences between euphotic and surface waters, represents an important goal for scientists and oceanic environmental managers. The monthly and seasonal dynamics in this study indicated that high phytoplankton biomass in the cold season and typhoon disturbance could play an important role in increasing oceanic phytoplankton biomass and/or production, particularly in oligotrophic environments such as the SCS. Our interannual and decadal observations showed a progressive increase in SST and decrease in MLD, averaged IChl-a and SChl-a concentrations. The phytoplankton biomass/production decreases with the shallowing of MLD and can be expected to continuously decrease with the current speed of global warming and climate change, hence reflecting the importance of having a long-term time-series station to monitor long-term oceanic environmental changes. Most importantly, given that the surface estimates are likely to bias the understandings of real oceanic phytoplankton biomass and/or productivity, measurements of phytoplankton responses in the euphotic zone may still not be simply replaced

by satellite remote sensing development. To better address contemporary environmental disruption, putting effort into long-term in situ monitoring remains essential for clarifying and overcoming concerns about environmental damage and climatic changes, as both IChl-a and MLD measurements can serve as alternative effective indicators.

Data Availability Statement

The data for this research can be found at http://140.112.70.58:5000/sharing/EWWB1Rb6W. The bathymetric map of the SCS was generated using GMT (Generic Mapping Tools). The typhoon records were compiled from the National Institute of Informatics (agora.ex.nii.ac.jp) from 2009 to 2018. Ocean eddies and meandering fronts were downloaded from Ocean Data Bank funded by the Ministry of Science and Technology (MOST), Taiwan (http://www.odb.ntu.edu.tw/). ENSO events, represented by MEI and ONI indices were downloaded from NOAA/National Weather Service (http://www.cpc.ncep.noaa.gov/and http://www.esrl.noaa.gov/psd/enso/mei/).

References

Alford, M. H., Peacock, T., MacKinnon, J. A., Nash, J. D., Buijsman, M. C., Centurioni, L. R., et al. (2015). The formation and fate of internal waves in the South China Sea. *Nature*, *521*(7550), 65–69. https://doi.org/10.1038/nature14399

Austria, E., Lai, C.-C., KoKo, C.-Y., Lee, K.-Y., Kuo, H.-Y., Chen, T.-Y., & Shiah, F.-K. (2018). Growth controlling mechanisms on heterotrophic bacteria in the South China Sea shelf: Summer and winter patterns. *Terrestrial, Atmospheric and Oceanic Sciences*, *29*(4), 1–13. https://doi.org/10.3319/tao.2018.01.19.01

Behrenfeld, M. J., & Falkowski, P. G. (1997). Photosynthetic rates derived from satellite-based chlorophyll concentration. *Limnology & Oceanography*, *42*(1), 1–20. https://doi.org/10.4319/lo.1997.42.1.0001

Boyce, D. G., Lewis, M. R., & Worm, B. (2010). Global phytoplankton decline over the past century. *Nature*, *466*(7306), 591–596. https://doi.org/10.1038/nature09268

Calbet, A., Agersted, M. D., Kaartvedt, S., Møhl, M., Møller, E. F., Poulsen, S. E., et al. (2015). Heterogeneous distribution of plankton within the mixed layer and its implications for bloom formation in tropical seas. *Scientific Reports*, *5*(1), 11240. https://doi.org/10.1038/srep11240

Carlson, C. A., Ducklow, H. W., & Michaels, A. F. (1994). Annual flux of dissolved organic carbon from the euphotic zone in the northwestern Sargasso Sea. *Nature*, *371*(6496), 405–408. https://doi.org/10.1038/371405a0

Chavez, F. P., Messie, M., & Pennington, J. T. (2011). Marine primary production in relation to climate variability and change. *Annual Review of Marine Science*, *3*(1), 227–260. https://doi.org/10.1146/annurev.marine.010908.163917

Chen, C.-C., Shiah, F.-K., Chung, S.-W., & Liu, K.-K. (2006). Winter phytoplankton blooms in the shallow mixed layer of the South China Sea enhanced by upwelling. *Journal of Marine Systems*, *59*(1–2), 97–110. https://doi.org/10.1016/j.jmarsys.2005.09.002

Claustre, H., Morel, A., Babin, M., Cailliau, C., Marie, D., Marty, J.-C., et al. (1999). Variability in particle attenuation and chlorophyll fluorescence in the tropical Pacific: Scales, patterns, and biogeochemical implications. *Journal of Geophysical Research*, *104*(C2), 3401–3422. https://doi.org/10.1029/98jc01334

Cullen, J. J. (2015). Subsurface chlorophyll maximum layers: Enduring enigma or mystery solved?*Annual Review of Marine Science*, *7*(1), 207–239. https://doi.org/10.1146/annurev-marine-010213-135111

Dall'Olmo, G., Dingle, J., Polimene, L., Brewin, R. J., & Claustre, H. (2016). Substantial energy input to the mesopelagic ecosystem from the seasonal mixed-layer pump. *Nature Geoscience*, *9*(11), 820–823. https://doi.org/10.1038/ngeo2818

Dall'Olmo, G., & Mork, K. A. (2014). Carbon export by small particles in the Norwegian Sea. *Geophysical Research Letters*, *41*(8), 2921–2927. https://doi.org/10.1002/2014gl059244

Falkowski, P. G., & Raven, J. A. (2013). *Aquatic photosynthesis*. Princeton University Press.

Field, C. B., Behrenfeld, M. J., Randerson, J. T., & Falkowski, P. J. S. (1998). Primary production of the biosphere: Integrating terrestrial and oceanic components. *Science*, *281*(5374), 237–240. https://doi.org/10.1126/science.281.5374.237

Frolov, S., Ryan, J., & Chavez, F. (2012). Predicting euphotic depth integrated chlorophyll-a from discrete depth and satellite observable chlorophyll-a off central California. *Journal of Geophysical Research*, *117*(C5). https://doi.org/10.1029/2011jc007322

Gardner, W. D., Chung, S. P., Richardson, M. J., & Walsh, I. D. (1995). The oceanic mixed-layer pump. *Deep Sea Research Part II: Topical Studies in Oceanography*, *42*(2–3), 757–775. https://doi.org/10.1016/0967-0645(95)00037-q

Gittings, J. A., Raitsos, D. E., Krokos, G., & Hoteit, I. (2018). Impacts of warming on phytoplankton abundance and phenology in a typical tropical marine ecosystem. *Scientific Reports*, *8*(1), 1–12. https://doi.org/10.1038/s41598-018-20560-5

Gordon, H. R., Clark, D. K., Mueller, J. L., & Hovis, W. A. (1980). Phytoplankton pigments from the Nimbus-7 Coastal Zone Color Scanner: Comparisons with surface measurements. *Science*, *210*(4465), 63–66. https://doi.org/10.1126/science.210.4465.63

Gregg, W. W. (2008). Assimilation of SeaWiFS ocean chlorophyll data into a three-dimensional global ocean model. *Journal of Marine Systems*, *69*(3–4), 205–225. https://doi.org/10.1016/j.jmarsys.2006.02.015

Hadfield, M. G., & Sharples, J. (1996). Modelling mixed layer depth and plankton biomass off the west coast of South Island, New Zealand. *Journal of Marine Systems*, *8*(1–2), 1–29. https://doi.org/10.1016/0924-7963(95)00045-3

Ho, C., & Marra, J. (1994). Early-spring export of phytoplankton production in the northeast Atlantic Ocean. *Marine Ecology: Progress Series*, *114*, 197–202. https://doi.org/10.3354/meps114197

Ho, T.-Y., Pan, X., Yang, H.-H., Wong, G. T. F., & Shiah, F.-K. (2015). Controls on temporal and spatial variations of phytoplankton pigment distribution in the Northern South China Sea. *Deep Sea Research Part II: Topical Studies in Oceanography*, *117*, 65–85. https://doi.org/10.1016/j.dsr2.2015.05.015

IPCC. (2013). *Climate Change 2013: The Physical Science Basis. Contribution of Working Group I to the Fifth Assessment Report of the Intergovernmental Panel on Climate Change* (In T. F. Stocker, D. Qin, G.-K. Plattner, M. Tignor, S. K. Allen, J. Boschung (Eds.), et al., Eds., p. 1535). Cambridge University Press.

Jeronimo, G., & Gomez-Valdes, J. (2010). Mixed layer depth variability in the tropical boundary of the California Current, 1997–2007. *Journal of Geophysical Research*, *115*(C5), C05014. https://doi.org/10.1029/2009jc005457

Karl, D. M., & Church, M. J. (2014). Microbial oceanography and the Hawaii Ocean Time-series programme. *Nature Reviews Microbiology*, *12*(10), 699–713. https://doi.org/10.1038/nrmicro3333

Ko, C.-Y., Lai, C.-C., Hsu, H.-H., & Shiah, F.-K. (2017). Decadal phytoplankton dynamics in response to episodic climatic disturbances in a subtropical deep freshwater ecosystem. *Water Research*, *109*, 102–113. https://doi.org/10.1016/j.watres.2016.11.011

Ko, D. S., Chao, S.-Y., Wu, C.-C., & Lin, I. I. (2014). Impacts of typhoon Megi (2010) on the South China Sea. *Journal of Geophysical Research: Oceans*, *119*(7), 4474–4489. https://doi.org/10.1002/2013jc009785

Lacour, L., Briggs, N., Claustre, H., Ardyna, M., & Dall'Olmo, G. (2019). The intraseasonal dynamics of the mixed layer pump in the subpolar North Atlantic Ocean: A Biogeochemical-Argo float approach. *Global Biogeochemical Cycles*, *33*(3), 266–281. https://doi.org/10.1029/2018gb005997

Lee, Z., & Carder, K. L. (2004). Absorption spectrum of phytoplankton pigments derived from hyperspectral remote-sensing reflectance. *Remote Sensing of Environment*, *89*(3), 361–368. https://doi.org/10.1016/j.rse.2003.10.013

Letelier, R. M., Bidigare, R. R., Hebel, D. V., Ondrusek, M., Winn, C. D., & Karl, D. M. (1993). Temporal variability of phytoplankton community structure based on pigment analysis. *Limnology & Oceanography*, *38*(7), 1420–1437. https://doi.org/10.4319/lo.1993.38.7.1420

Lin, I., Liu, W. T., Wu, C.-C., Wong, G. T. F., Hu, C., Chen, Z., et al. (2003). New evidence for enhanced ocean primary production triggered by tropical cyclone. *Geophysical Research Letters*, *30*(13). https://doi.org/10.1029/2003gl017141

Liu, K.-K., Chao, S.-Y., Shaw, P.-T., Gong, G.-C., Chen, C.-C., & Tang, T. (2002). Monsoon-forced chlorophyll distribution and primary production in the South China Sea: Observations and a numerical study. *Deep Sea Research Part I: Oceanographic Research Papers*, *49*(8), 1387–1412. https://doi.org/10.1016/s0967-0637(02)00035-3

Liu, K.-K., Wang, L. W., Dai, M., Tseng, C. M., Yang, Y., Sui, C. H., et al. (2013). Inter-annual variation of chlorophyll in the northern South China Sea observed at the SEATS Station and its asymmetric responses to climate oscillation. *Biogeosciences*, *10*(11), 7449–7462. https://doi.org/10.5194/bg-10-7449-2013

Liu, M., Liu, X., Ma, A., Zhang, B., & Jin, M. (2015). Spatiotemporal variability of chlorophyll a and sea surface temperature in the northern South China Sea from 2002 to 2012. *Canadian Journal of Remote Sensing*, *41*(6), 547–560. https://doi.org/10.1080/07038992.2015.1112728

Ma, S., Tao, Z., Yang, X., Yu, Y., Zhou, X., Ma, W., & Li, Z. (2014). Estimation of marine primary productivity from satellite-derived phytoplankton absorption data. *IEEE Journal of Selected Topics in Applied Earth Observations and Remote Sensing*, *7*(7), 3084–3092. https://doi.org/10.1109/jstars.2014.2298863

Marañón, E., Behrenfeld, M. J., González, N., Mouriño, B., & Zubkov, M. V. (2003). High variability of primary production in oligotrophic waters of the Atlantic Ocean: Uncoupling from phytoplankton biomass and size structure. *Marine Ecology Progress Series*, *257*, 1–11. https://doi.org/10.3354/meps257001

McClain, C. R. (2009). A decade of satellite ocean color observations. *Annual Review of Marine Science*, *1*, 19–42. https://doi.org/10.1146/annurev.marine.010908.163650

Mignot, A., Claustre, H., Uitz, J., Poteau, A., D'Ortenzio, F., & Xing, X. (2014). Understanding the seasonal dynamics of phytoplankton biomass and the deep chlorophyll maximum in oligotrophic environments: A Bio-Argo float investigation. *Global Biogeochemical Cycles*, *28*(8), 856–876. https://doi.org/10.1002/2013gb004781

Morel, A., & Berthon, J.-F. (1989). Surface pigments, algal biomass profiles, and potential production of the euphotic layer: Relationships reinvestigated in view of remote-sensing applications. *Limnology & Oceanography*, *34*(8), 1545–1562. https://doi.org/10.4319/lo.1989.34.8.1545

Murray, A. P., Gibbs, C. F., Longmore, A. R., & Flett, D. J. (1986). Determination of chlorophyll in marine waters: Intercomparison of a rapid HPLC method with full HPLC, spectrophotometric and fluorometric methods. *Marine Chemistry*, *19*(3), 211–227. https://doi.org/10.1016/0304-4203(86)90024-1

Neveux, J. (2003). Diel dynamics of chlorophylls in high-nutrient, low-chlorophyll waters of the equatorial Pacific (180°): Interactions of growth, grazing, physiological responses, and mixing. *Journal of Geophysical Research*, *108*(C12), 8140. https://doi.org/10.1029/2000jc000747

Oka, A., & Niwa, Y. (2013). Pacific deep circulation and ventilation controlled by tidal mixing away from the sea bottom. *Nature Communications*, *4*(1), 1–8. https://doi.org/10.1038/ncomms3419

Owen, R. W. (1981). Fronts and eddies in the sea: Mechanisms, interactions and biological effects. In A. R.Longhurst (Ed.), *Analysis of Marine Ecosystems* (pp. 197–233). Academic Press.

Pan, X., Wong, G. T. F., Tai, J.-H., & Ho, T.-Y. (2015). Climatology of physical hydrographic and biological characteristics of the Northern South China Sea Shelf-sea (NoSoCS) and adjacent waters: Observations from satellite remote sensing. *Deep Sea Research Part II: Topical Studies in Oceanography*, *117*, 10–22. https://doi.org/10.1016/j.dsr2.2015.02.022

Pauly, D., & Liang, C. (2020). The fisheries of the South China Sea: Major trends since 1950. *Marine Policy*, *121*, 103584. https://doi.org/10.1016/j.marpol.2019.103584

Pörtner, H.-O., Karl, D. M., Boyd, P. W., Cheung, W., Lluch-Cota, S. E., Nojiri, Y., et al. (2014). Ocean systems. In C. B.Field, V. R.Barros, D. J.Dokken, K. J.Mach, M. D.Mastrandrea, T. E.Bilir, et al. (Eds.), *Climate Change 2014: Impacts, Adaptation, And Vulnerability. Part A: Global and Sectoral Aspects. Contribution of Working Group II to the Fifth Assessment Report of the Intergovernmental Panel on Climate Change* (pp. 411–484). Cambridge University Press.

Price, J. F., Weller, R. A., & Pinkel, R. (1986). Diurnal cycling: Observations and models of the upper ocean response to diurnal heating, cooling, and wind mixing. *Journal of Geophysical Research*, *91*(C7), 8411–8427. https://doi.org/10.1029/jc091ic07p08411

Qiu, Y., Lin, Z., & Wang, Y. (2010). Responses of fish production to fishing and climate variability in the northern South China Sea. *Progress in Oceanography*, *85*(3–4), 197–212. https://doi.org/10.1016/j.pocean.2010.02.011

Rasconi, S., Gall, A., Winter, K., & Kainz, M. J. (2015). Increasing water temperature triggers dominance of small freshwater plankton. *PLoS One*, *10*(10), e0140449. https://doi.org/10.1371/journal.pone.0140449

R Core Team. (2019). *R: A language and environment for statistical computing*. R Foundation for Statistical Computing. Retrieved from https://www.R-project.org/

Saba, V. S., Friedrichs, M. A., Carr, M. E., Antoine, D., Armstrong, R. A., Asanuma, I., et al. (2010). Challenges of modeling depth-integrated marine primary productivity over multiple decades: A case study at BATS and HOT. *Global Biogeochemical Cycles*, *24*(3). https://doi.org/10.1029/2009gb003655

Schofield, O., Brown, M., Kohut, J., Nardelli, S., Saba, G., Waite, N., & Ducklow, H. (2018). Changes in the upper ocean mixed layer and phytoplankton productivity along the West Antarctic Peninsula. *Philosophical Transactions of the Royal Society A*, *376*(2122), 20170173. https://doi.org/10.1098/rsta.2017.0173

Schollaert Uz, S., Busalacchi, A. J., Smith, T. M., Evans, M. N., Brown, C. W., & Hackert, E. C. (2017). Interannual and decadal variability in tropical Pacific chlorophyll from a statistical reconstruction: 1958–2008. *Journal of Climate*, *30*(18), 7293–7315. https://doi.org/10.1175/jcli-d-16-0202.1

Shaw, P.-T., & Chao, S.-Y. (1994). Surface circulation in the South China Sea. *Deep Sea Research Part I: Oceanographic Research Papers*, *41*(11–12), 1663–1683. https://doi.org/10.1016/0967-0637(94)90067-1

Siegel, D. A., Behrenfeld, M. J., Maritorena, S., McClain, C. R., Antoine, D., Bailey, S. W., et al. (2013). Regional to global assessments of phytoplankton dynamics from the SeaWiFS mission. *Remote Sensing of Environment*, *135*, 77–91. https://doi.org/10.1016/j.rse.2013.03.025

Siegel, D. A., Dickey, T., Washburn, L., Hamilton, M. K., & Mitchell, B. (1989). Optical determination of particulate abundance and production variations in the oligotrophic ocean. *Deep Sea Research Part I: Oceanographic Research Papers*, *36*(2), 211–222. https://doi.org/10.1016/0198-0149(89)90134-9

Sirevaag, A., de la Rosa, S., Fer, I., Nicolaus, M., Tjernstrom, M., & McPhee, M. G. (2011). Mixing, heat fluxes and heat content evolution of the Arctic Ocean mixed layer. *Ocean Science*, *7*(3), 335–349. https://doi.org/10.5194/os-7-335-2011

Somavilla, R., Gonzalez-Pola, C., & Fernandez-Diaz, J. (2017). The warmer the ocean surface, the shallower the mixed layer. How much of this is true? *Journal of Geophysical Research: Oceans*, *122*(9), 7698–7716. https://doi.org/10.1002/2017jc013125

Strickland, J. D., & Parsons, T. R. (1972). *A practical handbook of seawater analysis* (pp. 185–205). Bulletin Fisheries Research Board of Canada.

Tai, J.-H., Wong, G. T. F., & Pan, X. (2017). Upper water structure and mixed layer depth in tropical waters: The SEATS station in the northern South China Sea. *Terrestrial, Atmospheric and Oceanic Sciences*, *28*(6), 1019–1032. https://doi.org/10.3319/tao.2017.01.09.01

Tatebe, H., Tanaka, Y., Komuro, Y., & Hasumi, H. (2018). Impact of deep ocean mixing on the climatic mean state in the Southern Ocean. *Scientific Reports*, *8*(1), 1–9. https://doi.org/10.1038/s41598-018-32768-6

Toseland, A., Daines, S. J., Clark, J. R., Kirkham, A., Strauss, J., Uhlig, C., et al. (2013). The impact of temperature on marine phytoplankton resource allocation and metabolism. *Nature Climate Change*, *3*(11), 979–984. https://doi.org/10.1038/nclimate1989

Tseng, C.-M., Wong, G. T. F., Lin, I.-I., Wu, C.-R., & Liu, K.-K. (2005). A unique seasonal pattern in phytoplankton biomass in low-latitude waters in the South China Sea. *Geophysical Research Letters*, *32*(8), L08608. https://doi.org/10.1029/2004gl022111

Uitz, J., Claustre, H., Morel, A., & Hooker, S. B. (2006). Vertical distribution of phytoplankton communities in open ocean: An assessment based on surface chlorophyll. *Journal of Geophysical Research*, *111*(C8), C08005. https://doi.org/10.1029/2005jc003207

Vanharanta, M., Elovaara, S., Franklin, D. J., Spilling, K., & Tamelander, T. (2020). Viability of pico-and nanophytoplankton in the Baltic Sea during spring. *Aquatic Ecology*, *54*(1), 119–135. https://doi.org/10.1007/s10452-019-09730-3

Vaulot, D., & Marie, D. (1999). Diel variability of photosynthetic picoplankton in the equatorial Pacific. *Journal of Geophysical Research*, *104*(C2), 3297–3310. https://doi.org/10.1029/98jc01333

Winder, M., & Sommer, U. (2012). Phytoplankton response to a changing climate. *Hydrobiologia*, *698*(1), 5–16. https://doi.org/10.1007/978-94-007-5790-5_2

Wong, G. T. F., Ku, T.-L., Liu, H., & Mulholland, M. (2015). The oceanography of the Northern south China Sea Shelf-Sea (NoSoCS) and its adjacent waters-overview and highlights. *Deep-Sea Research II: Topical Studies in Oceanography*, *117*, 3–9. https://doi.org/10.1016/j.dsr2.2015.04.026

Woods, J., & Onken, R. (1982). Diurnal variation and primary production in the ocean preliminary results of a Lagrangian ensemble model. *Journal of Plankton Research*, *4*(3), 735–756. https://doi.org/10.1093/plankt/4.3.735

Wu, J., Chung, S.-W., Wen, L.-S., Liu, K.-K., Chen, Y.-l. L., Chen, H.-Y., & Karl, D. M. (2003). Dissolved inorganic phosphorus, dissolved iron, and *Trichodesmium* in the oligotrophic South China Sea. *Global Biogeochemical Cycles*, *17*(1), 8-1–8-10. https://doi.org/10.1029/2002gb001924

Xian, T., Sun, L., Yang, Y.-J., & Fu, Y.-F. (2012). Monsoon and eddy forcing of chlorophyll-a variation in the northeast South China Sea. *International Journal of Remote Sensing*, *33*(23), 7431–7443. https://doi.org/10.1080/01431161.2012.685970

Ye, H., Kalhoro, M. A., Morozov, E., Tang, D., Wang, S., & Thies, P. R. (2017). Increased chlorophyll-a concentration in the South China Sea caused by occasional sea surface temperature fronts at peripheries of eddies. *International Journal of Remote Sensing*, *39*(13), 4360–4375. https://doi.org/10.1080/01431161.2017.1399479

Zhao, H., Tang, D., & Wang, Y. (2008). Comparison of phytoplankton blooms triggered by two typhoons with different intensities and translation speeds in the South China Sea. *Marine Ecology Progress Series*, *365*, 57–65. https://doi.org/10.3354/meps07488